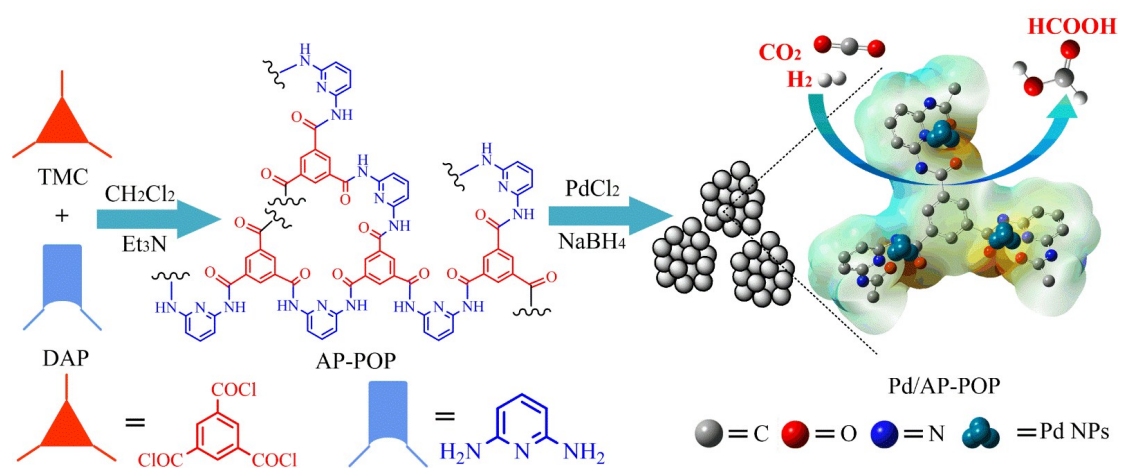


Supporting Information

Efficient synthesis of highly dispersed ultrafine Pd nanoparticles on a porous organic polymer for hydrogenation of CO₂ to formic acid

Xianzhao Shao,^{a,*} Xinyi Miao,^a Xiaohu Yu,^a Wei Wang,^a Xiaohui Ji,^a

^aShaanxi Key Laboratory of Catalysis, School of Chemistry and Environment
Science, Shaanxi University of Technology, Hanzhong 723001, Shaanxi, China



Scheme S1. Synthetic route for Pd/AP-POP catalyst.

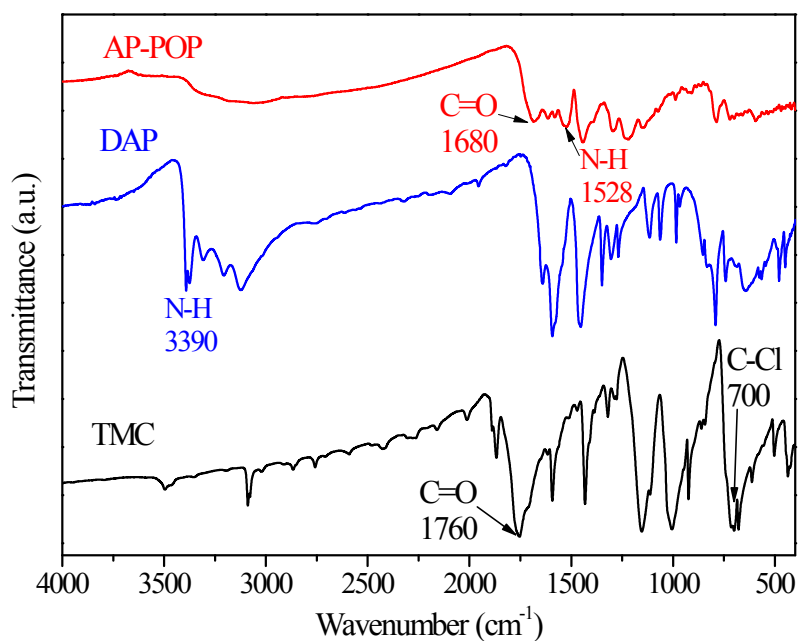


Figure S1. FT-IR spectra of the AP-POP, 1,3,5-benzenetricarbonyl chloride (TMC) and 2,6-diaminopyridine (DAP). The absorption bands in between 1680 cm^{-1} correspond to the amide C=O stretching frequency, also known as amide-I band. The band observed in the range 1528 cm^{-1} corresponds to NH bending vibration, called amide-II band. No acid chloride (700 cm^{-1}) and amine bands corresponding to the starting compounds appear, demonstrating the complete transformation of starting material to polyamide POPs.

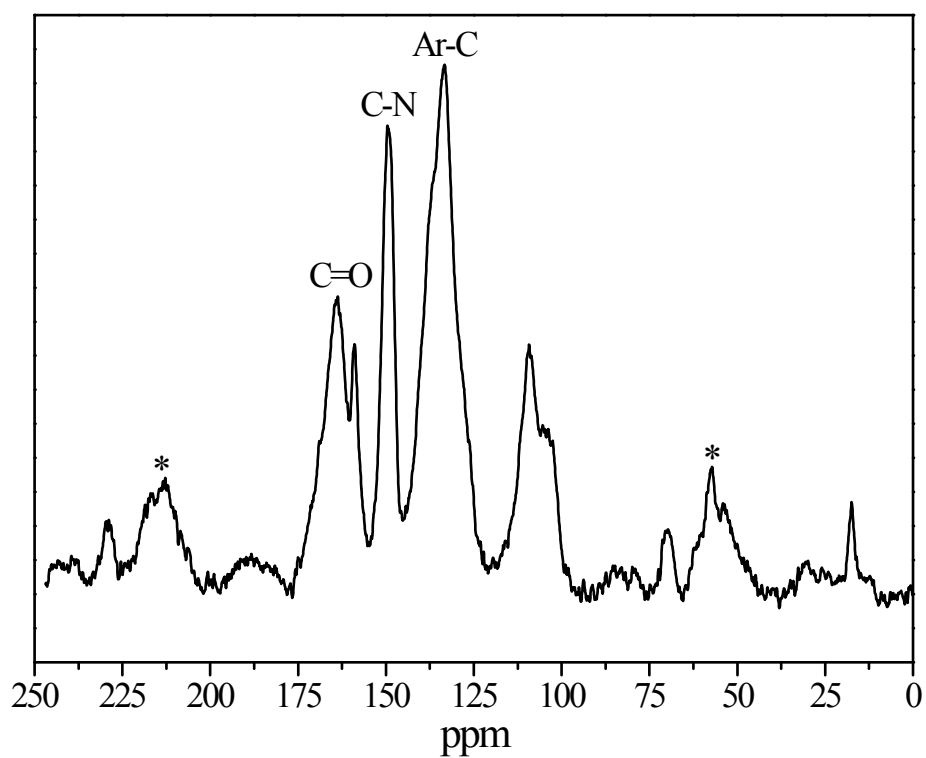


Figure S2. The ^{13}C CP-MAS solid state NMR spectra of AP-POP. A signal at 164 ppm corresponds to the amide carbonyl. The overlapping signals between 109 and 150 ppm correspond to the aromatic carbons from phenyl and pyridyl moieties. * indicates peaks arising from spinning side bands.

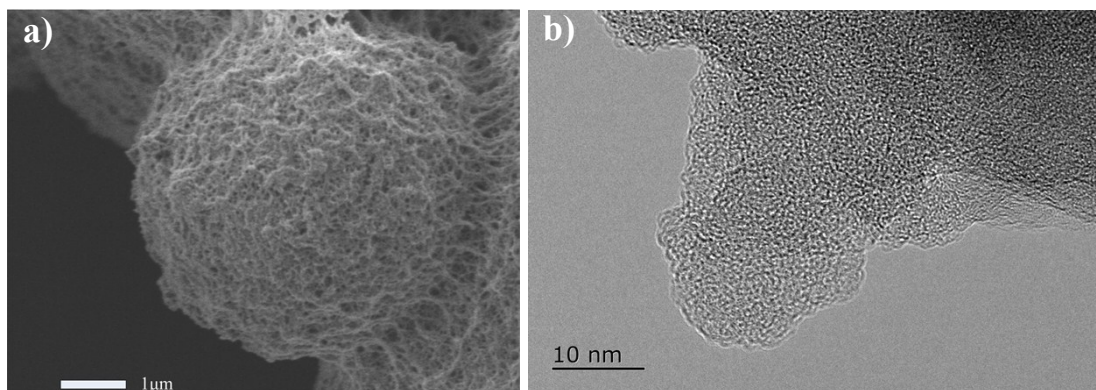


Figure S3. SEM and TEM images of AP-POP.

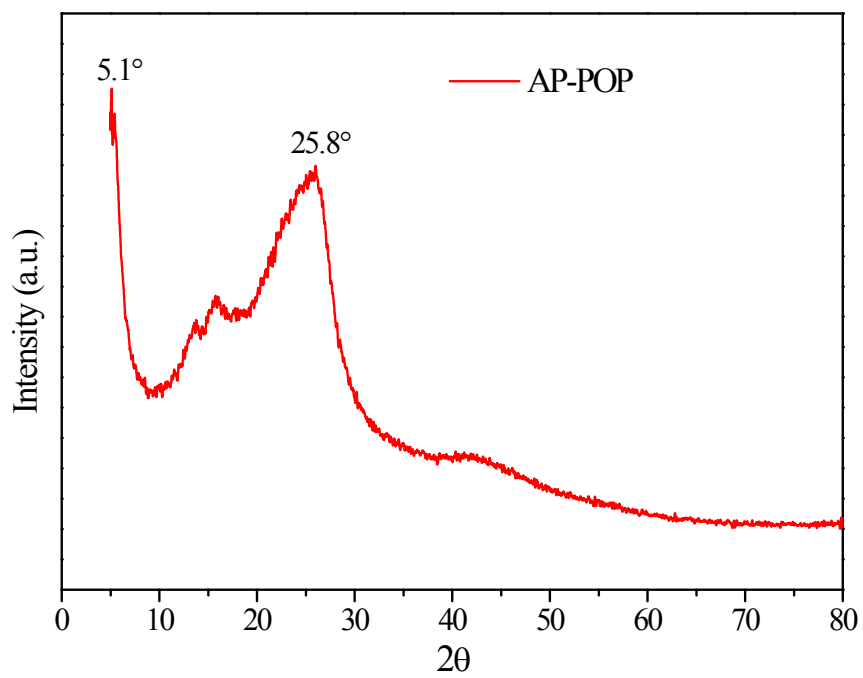


Figure S4. The X-ray powder diffraction (XRPD) patterns of AP-POP.

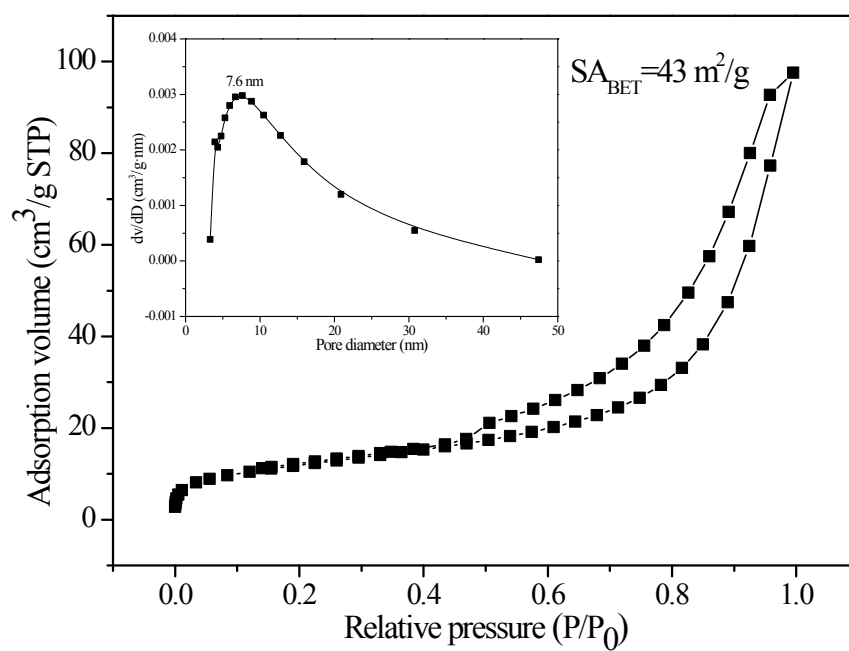


Figure S5. N₂ adsorption/desorption isotherms of the AP-POP at 77 K (inset: pore size distribution curves of the AP-POP).

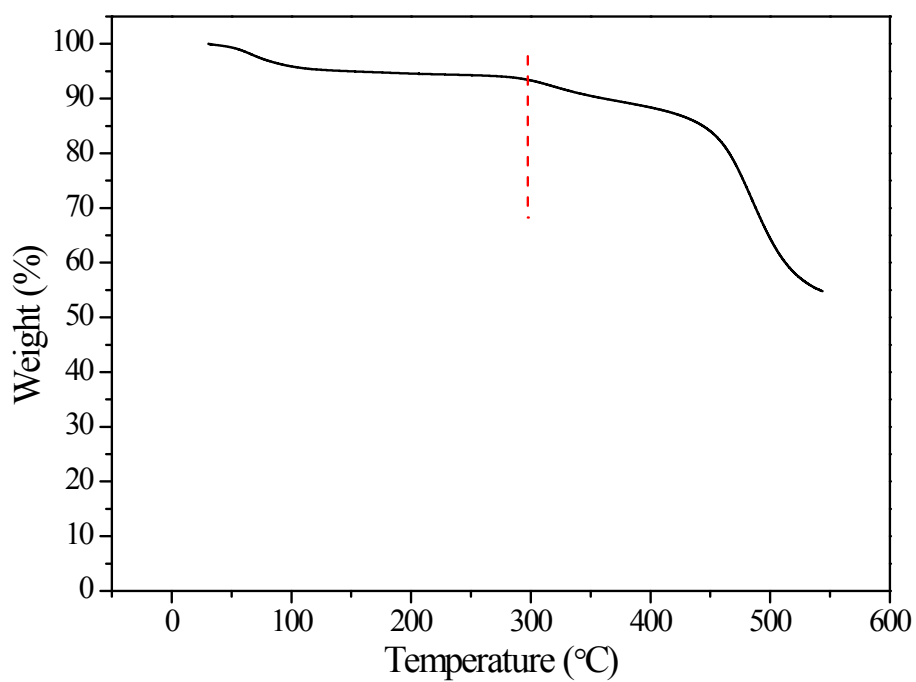


Figure S6. Thermogravimetric analysis (TGA) data of AP-POP. The initial weight loss [$\sim 8\%$] of AP-POP in TGA corresponds to the loss of trapped solvent as well as the moisture in the pores. The framework decomposition occurs above $300\text{ }^{\circ}\text{C}$ with a gradual weight loss of 40% .

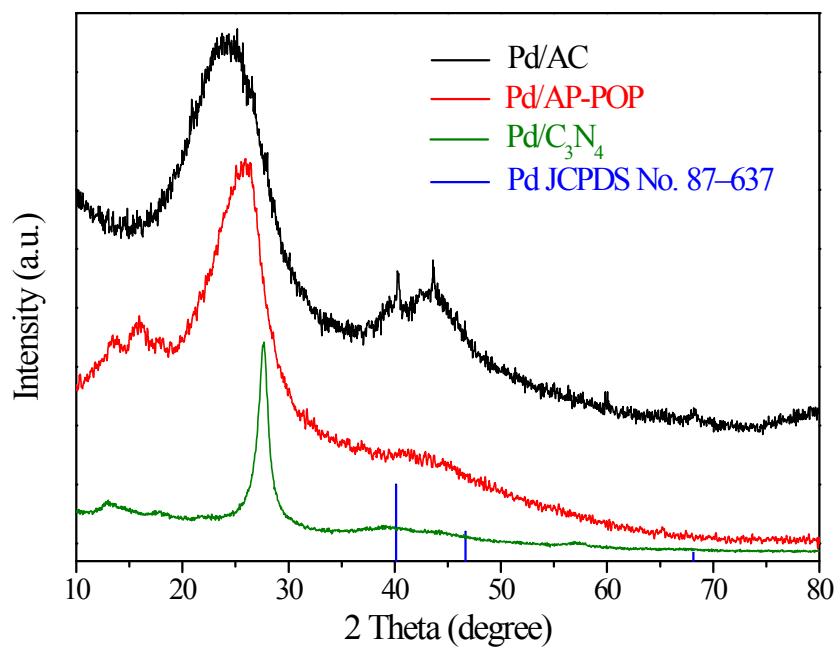


Figure S7. XRD patterns of Pd/AP-POP, Pd/AC and Pd/C₃N₄ catalysts.

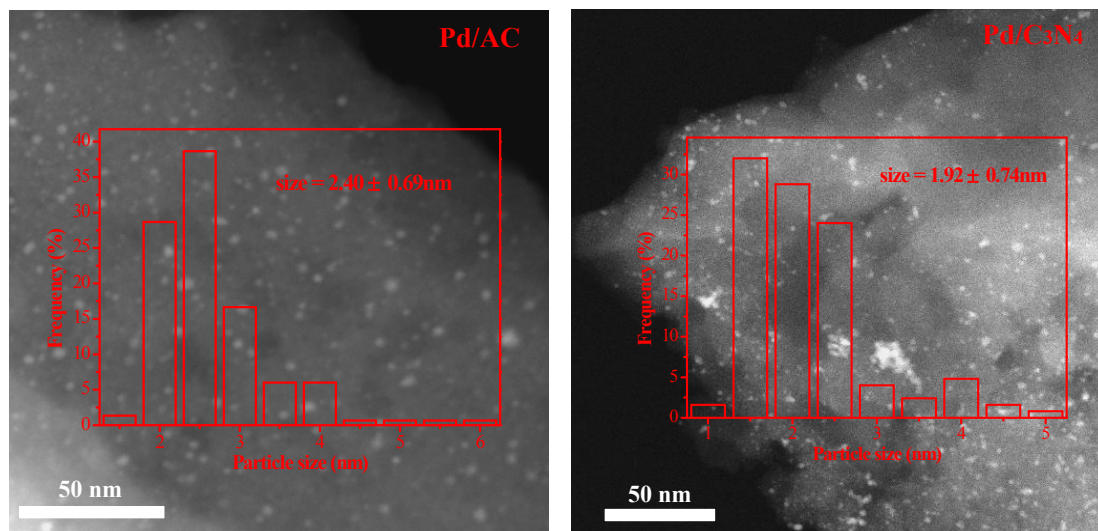


Figure S8. TEM images of the Pd/AC and Pd/C₃N₄ catalysts with the Pd NP size distribution.

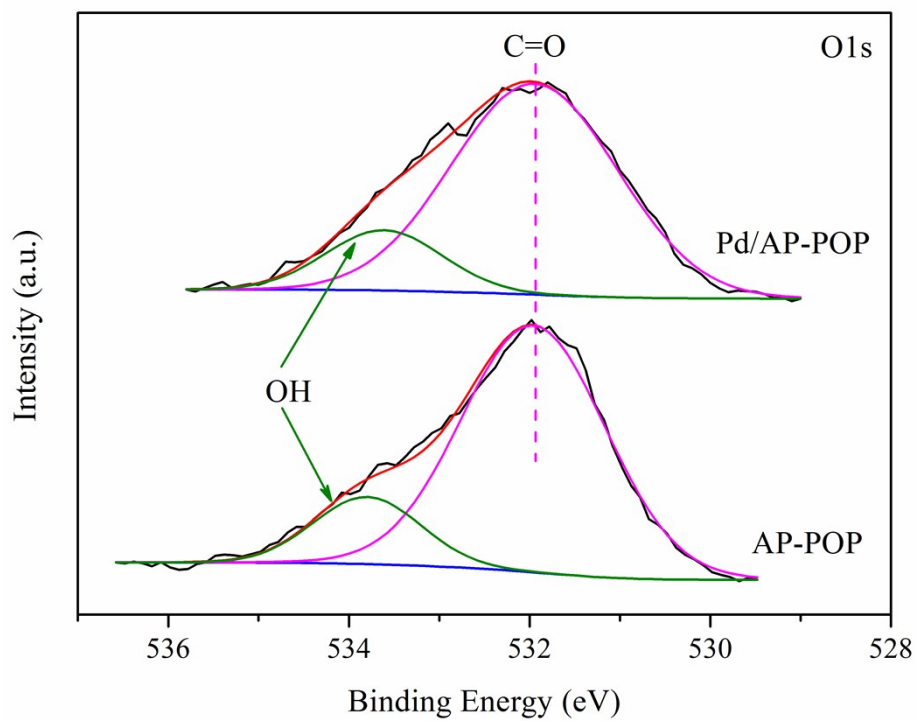


Figure S9. The high-resolution spectrum of O 1s of AP-POP and Pd/AP-POP.

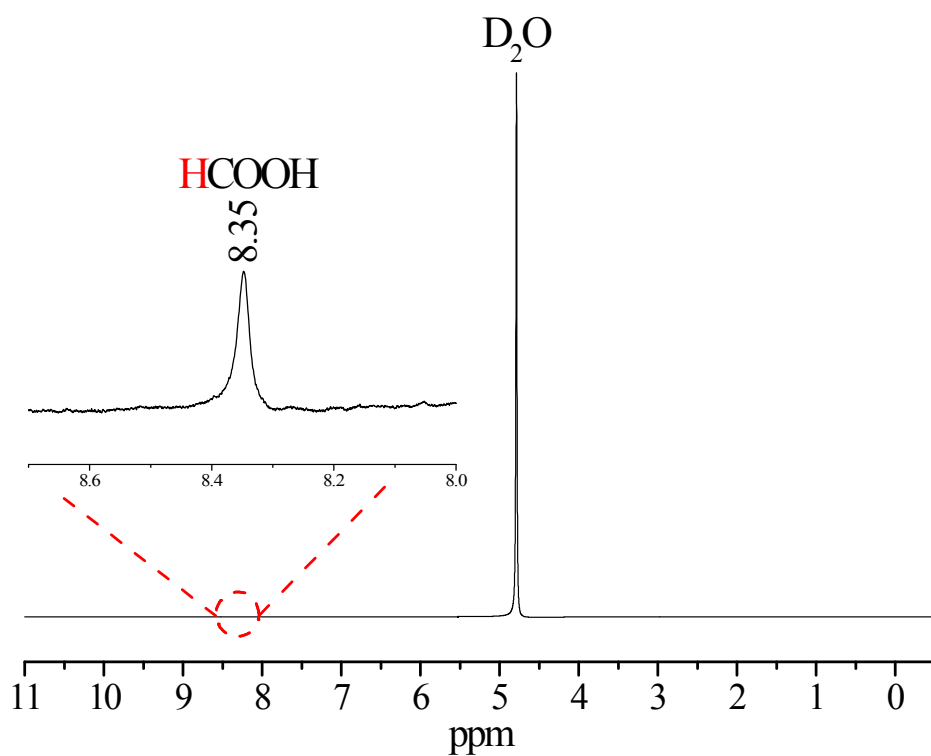
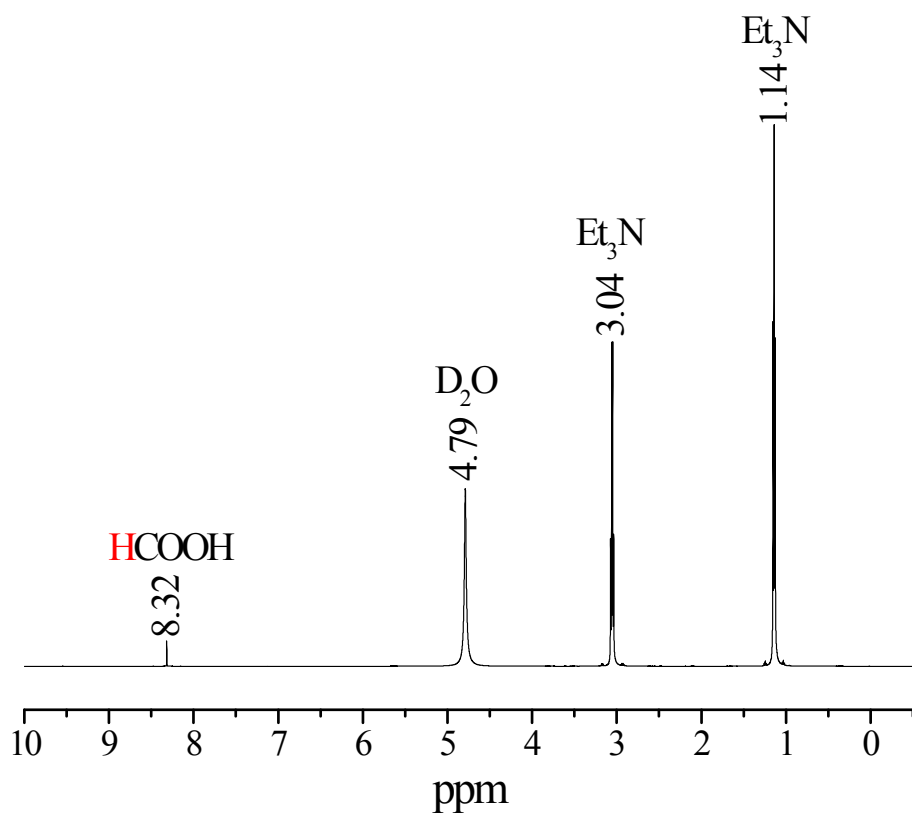


Figure S10. ^1H NMR spectra of a reaction mixture after CO_2 reduction (with and without Et_3N).

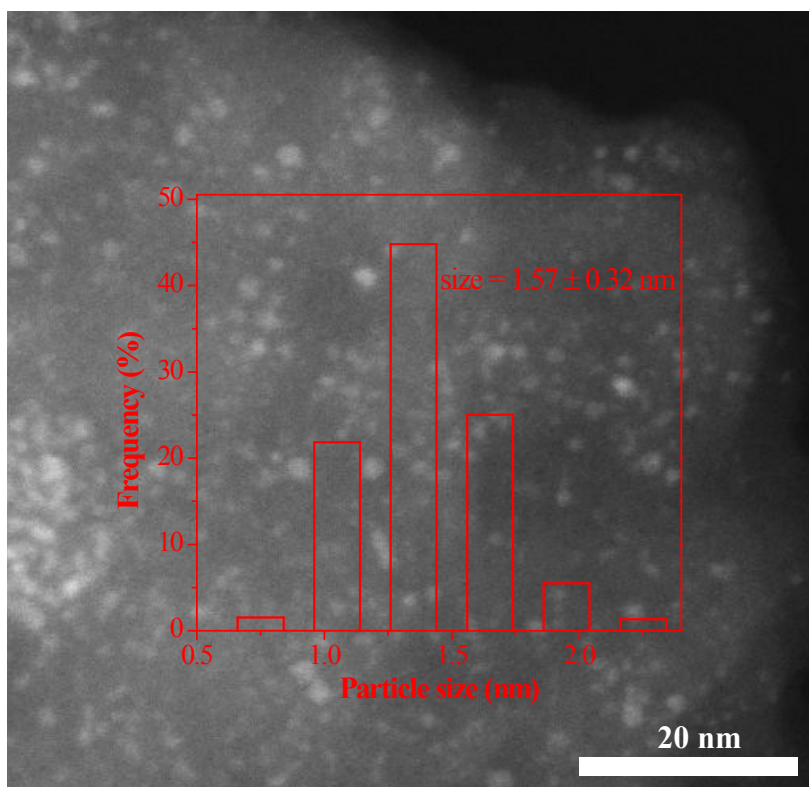


Figure S11. STEM images of the used Pd/AP-POP catalyst and Pd NP size distribution.

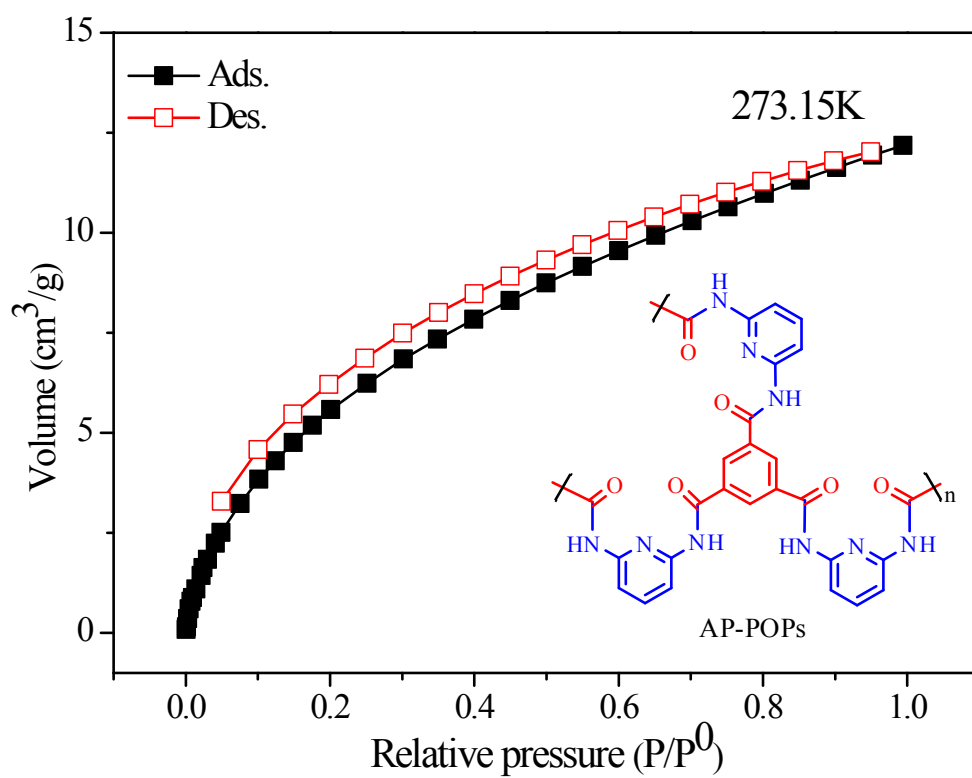


Figure S12. Carbon dioxide adsorption isotherms collected at 273 K for AP-POP.

Table S1. Chemical composition and textural properties of different materials.

Materials	Elemental analysis ^a (%)				$S_{\text{BET}}^{\text{b}}$ (m^2g^{-1})	Pore size ^c (nm)
	C	N	H	Pd		
AP-POP	57.96	17.75	4.22	none	43	7.8
Pd/AP-POP	56.85	16.32	3.97	3.5	16	10.7
C_3N_4	38.59	58.83	1.02	none	99	4.0
Pd/ C_3N_4	37.2	57.14	0.94	3.3	21	7.6
AC	76.5	0.65	1.9	none	631	2.8
Pd/AC	75.13	0.57	1.52	3.2	517	2.9

[a] Elemental analysis of C, H and N was carried out by using a PerkinElmer 2400 instrument. Pd content was quantified by ICP-OES. [b] Brunauer–Emmett–Teller (BET) method. [c] The average pore sizes calculated from the adsorption branch by using Barrett–Joyner–Halenda (BJH) method.

Table S2. Comparison of the activity in the transformation of CO₂ to FA in the pure water condition.

Catalysts	T [°C]	Time [h]	Pressure(H ₂ /CO ₂)	TON	TOF	Ref.
Pd/AP-POP	80	12	3.0/3.0 [MPa]	128	10.7	This work
PdAg/amine-RF10	40	24	2.0/2.0 [MPa]	63	2.6	1
PdNi/CNT	40	16	25/25 [bar]	3	0.2	2
0.6Pd/C ₃ N ₄	40	16	25/25 [bar]	24	1.5	3
2Pd/ECN	40	16	2.5/2.5 [MPa]	35	2.2	4
RuCl ₂ (PTA) ₄	60	16	25/25 [bar]	158	9.9	5

Reference

- [1] S. Masuda, K. Mori, Y. Kuwahara and H. Yamashita. *J. Mater. Chem. A*, **2019**, 7, 16356–16363.
- [2] L. T. M. Nguyen, H. Park, M. Banu, J. Y. Kim, D. H. Youn, G. Magesh, W. Y. Kim, and J. S. Lee, *RSC Adv.*, **2015**, 5, 105560–105566.
- [3] H. Park, J. H. Lee, E. H. Kim, K. Y. Kim, Y. H. Choi, D. H. Youn and J. S. Lee, *Chem. Commun.*, **2016**, 52, 14302–14305.
- [4] C. Mondelli, B. Purlas, M. Ackermann, Z. Chen and J. P. Ramírez, *ChemSusChem*, **2018**, 11, 2859–2869.
- [5] S. Moret, P. J. Dyson and G. Laurenczy, *Nat. Commun.*, **2014**, 5, 4017.